ISSN 1063-7761, Journal of Experimental and Theoretical Physics, 2021, Vol. 133, No. 5, pp. 574–580. © Pleiades Publishing, Inc., 2021.
Russian Text © The Author(s), 2021, published in Zhurnal Eksperimental'noi i Teoreticheskoi Fiziki, 2021, Vol. 160, No. 5, pp. 670–677.

ORDER, DISORDER, AND PHASE TRANSITION IN CONDENSED SYSTEM

EPR Study of the Single-Ion Magnetic Anisotropy of the Fe^{3+} Ion in a Diamagnetic $PbGaBO_4$ Crystal

A. M. Vorotynov[a,*], A. I. Pankrats[a,b,], and M. I. Kolkov[a]**

[a] *Kirensky Institute of Physics, Siberian Branch, Russian Academy of Sciences, Krasnoyarsk, 660036 Russia*
[b] *Siberian Federal University, Krasnoyarsk, 660041 Russia*
**e-mail: sasa@iph.krasn.ru*
***e-mail: pank@iph.krasn.ru*

Received June 29, 2021; revised July 12, 2021; accepted July 12, 2021

Abstract—Crystals of a diamagnetic $PbGaBO_4$ analog containing a small amount (about 0.5 at %) of Fe^{3+} ions are grown. The single-ion EPR spectra of Fe^{3+} in $PbGa_{1-x}Fe_xBO_4$ single crystals are analyzed with allowance for a crystal structure. The existence of four magnetically nonequivalent positions of Fe^{3+} ions with different local anisotropy axis directions has been confirmed. The parameters of the spin Hamiltonian written in the approximation of the local orthorhombic symmetry of a paramagnetic center are determined. The values of single-ion anisotropy constants, which are unusually high for S ions, is shown to be caused by a strong distortion of the ligand environment of Fe^{3+} ions. The single-ion contribution to the energy of the total magnetic anisotropy of a magnetically concentrated $PbGaBO_4$ crystal is estimated. Two-ion mechanisms of the Fe–Fe interaction anisotropy are assumed to play a dominant role in the formation of magnetic anisotropy in a magnetically concentrated crystal.

DOI: 10.1134/S1063776121110054

INTRODUCTION

Among the Pb-containing crystals, the family of orthoborates with the general formula $PbABO_4$ has recently attracted great interest. Their crystal structure for A = Ga or Al was investigated for the first time in [1, 2], where their orthorhombic structure with the space group *Pnma* was identified. The main structural elements of the crystals of this family are chains of edge-sharing oxygen octahedra, at the centers of which A^{3+} ions are located. The magnetic properties of the crystals of this family with A = Fe, Cr, and Mn were studied in the polycrystalline state by the same group of researchers [3], and an interesting feature of this family was discovered. Specifically, the type of magnetic order depends on paramagnetic ion A. Crystals with A = Fe or Cr were found to be antiferromagnets with Néel temperatures of 125 and 8.3 K, respectively. The compound with A = Mn was the only one with a ferromagnetic order in this series; this fact is unique, since a ferromagnetic order is extremely rare in oxide compounds. Studies on single crystals provide much more reliable information, since polycrystalline objects can contain foreign crystalline phases. We grew $PbFeBO_4$ single crystals using spontaneous solidification in a melt solution, and our studies [4] showed that the magnetic properties of the single crystals differed substantially from those of polycrystals. According to the refined data, the Néel temperature is 114 K, and the temperature dependence of the magnetic susceptibility is most likely to correspond to a three-dimensional model of the magnetic structure rather than to a quasi-one-dimensional model following from the polycrystalline data [3]. Magnetodielectric anomalies were also found in a $PbFeBO_4$ crystal in the magnetic order region, and they indicate the presence of a relation between the magnetic and dielectric subsystems of the crystal. Studies on single crystals have another advantage, allowing us to study the anisotropic properties of compounds. The studies of the magnetic and resonance properties of $PbMnBO_4$ single crystals grown by us [5] showed that this compound below the Curie temperature ($T_C = 30.3$ K) is a strongly anisotropic ferromagnet. As was shown in [5], the static Jahn–Teller effect causes the formation of both the ferromagnetic exchange coupling in chains of MnO_6 octahedra and the strong magnetic anisotropy of the crystal. The significant effective anisotropy fields of $PbMnBO_4$ determine an extremely large (for ferromagnets) energy gap in the FMR spectrum of crystal (112 GHz at $T = 4.2$ K). We [6] also found that, when the crystal is heated in the absence of an external magnetic field, a noticeable magnetic contribution to its heat capacity is retained up to the temperatures twice as high as T_C, and this range becomes even wider

Table 1. Charge composition used to grow a $PbGa_{1-x}Fe_xBO_4$ single crystal

	PbO, g	B_2O_3, g	Fe_2O_3, g	Ga_2O_3, g
$PbGa_{1-x}Fe_xBO_4$ ($x = 0.005$)	79.4	17.2	0.007	14.0493

in strong fields. This fact and the difference between T_C and paramagnetic Curie temperature $\Theta = 49$ K were explained by the influence of a chain character of the magnetic structure of the $PbMnBO_4$ crystal. An important structural feature of this family of crystals is the distorted oxygen octahedron surrounding an A^{3+} ion. These distortions are especially large in the case when a Jahn–Teller Mn^{3+} ion is located at the center of the octahedron, causing a strong magnetic anisotropy of the $PbMnBO_4$ crystal. Another important structural feature of $PbABO_4$ crystals is the noncollinearity of local octahedron distortion axes, which leads to noncollinear single-ion magnetic anisotropy axes of the crystal. It is this noncollinearity that brings about a new effect, namely, the orientation transition detected in the $PbMnBO_4$ crystal during magnetization along one of the orthorhombic axes [7–9]. The distortions of the oxygen environment of paramagnetic ions and the noncollinearity of the local distortion axes cause an important role of the single-ion magnetic anisotropy in crystals of the $PbABO_4$ family. Taking into account the fact that the oxygen environment of an iron ion in $PbFeBO_4$ also undergoes noticeable distortions, we can expect that the single-ion anisotropy in this crystal can also be significant. In particular, we [7] studied the magnetoanisotropic properties of the $PbMnBO_4$ crystal when Fe^{3+} ions partially substituted for Mn^{3+} ions. We expected that the magnetic anisotropy would decrease after this substitution, which would be quite logical for an S ion, i.e., Fe^{3+} ion. However, this substitution not only did not decrease the magnetic anisotropy, but even caused its enhancement and the corresponding increase in the gap in the FMR spectrum. Thus, the study of the single-ion magnetic anisotropy of a number of paramagnetic ions in the $PbABO_4$ family is an important and challenging problem. One of the most effective experimental methods for solving such a problem is to study single crystals of the diamagnetic analogs of this family containing small additions of paramagnetic ions in the octahedral positions of the crystal. The study of the single-ion EPR spectra of such ions and an analysis of these data in terms of a spin Hamiltonian make it possible to experimentally measure the single-ion anisotropy constants for the corresponding paramagnetic ions. The purpose of this work is to investigate the single-ion EPR spectrum of the Fe^{3+} ion in a diamagnetic $PbGaBO_4$ crystal. Orthoborate $PbGa_{1-x}Fe_xBO_4$ single crystals containing a small addition of Fe^{3+} ions were grown. When studying a single-ion EPR spectrum, we were able to determine the parameters of the spin Hamiltonian of the Fe^{3+} ion in a $PbGaBO_4$ single crystal. An unusually high (for S ion) single-ion magnetic anisotropy constant for the Fe^{3+} ion was found.

EXPERIMENTAL

$PbGaBO_4$ single crystals containing small (less than 1 at %) Fe^{3+} ion additives were grown using a modified method of pseudosolution–melt spontaneous solidification. To prevent possible contamination of the crystal with foreign impurities, the single crystals were synthesized using $PbO–B_2O_3$ oxides included in the chemical formula of the synthesized compound as solvents. The composition of the charge used to grow the single crystals is given in Table 1.

The single crystals were synthesized under the following technological conditions: a smooth rise to a temperature of 970°C in 5 h, holding for 4 h, and a slow decrease in the temperature down to 750°C at a rate of 3.20°C/h. After the furnace was turned off, the platinum crucible was retained in the furnace until it completely cooled down. The single crystals were mechanically extracted from the crucible. The transparent orange crystals are elongated prismatic needles with a cross section in the form of a flattened parallelogram $2 \times 0.2 \times 0.2$ mm^3 in size. X-ray diffraction (XRD) studies confirmed the orthorhombic space group *Pnma*, and the lattice parameters coincided with [1], namely, $a = 6.9944(10)$ Å, $b = 5.8925(8)$ Å, $c = 8.2495(11)$ Å, $V = 340.00(8)$ Å^3, and $Z = 4$. Figure 1 shows a general view of the crystal structure of $PbGa_{1-x}Fe_xBO_4$. The main structural element is represented by chains of edge-sharing oxygen octahedra, at the center of which a Ga^{3+} or Fe^{3+} ion is located. The chains are arranged along the orthorhombic b axis and are interconnected through BO_3 and PbO_4 groups. The exchange interaction through the PbO_4 group is likely to be fundamentally important. For example, the authors of [10] showed that the substitution of Sr for Pb changed the ferromagnetic interaction between the chains into antiferromagnetic.

The orientation and quality of the single crystals were determined using the Photonic Science Laue crystal orientation system. Figure 2 shows the Laue pattern of the $PbGa_{1-x}Fe_xBO_4$ single crystal; it formed upon reflection of a primary beam from one of the lateral crystal faces (which is a (101) diagonal plane). The absence of double and ring reflections confirms a high quality of the single crystal. Thus, according to XRD data, the orthorhombic b axis coincides with the long needle direction and the natural lateral crystal faces are (101) diagonal planes. In experiments, the crystal was oriented according to the natural faceted shape of the crystal. Electron para-

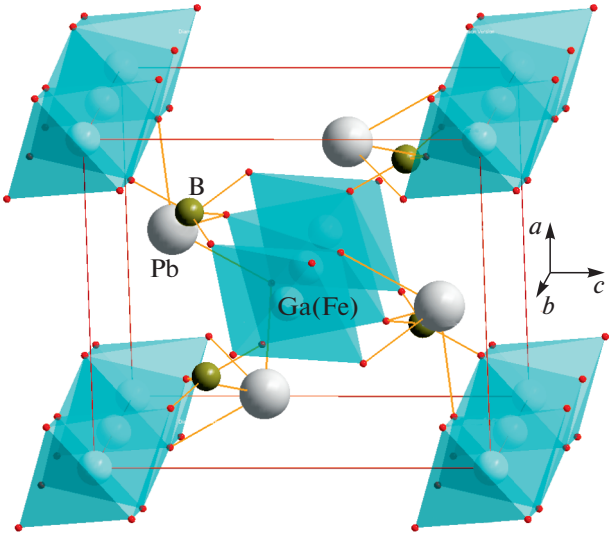

Fig. 1. General view of the crystal structure of $PbGa_{1-x}Fe_xBO_4$.

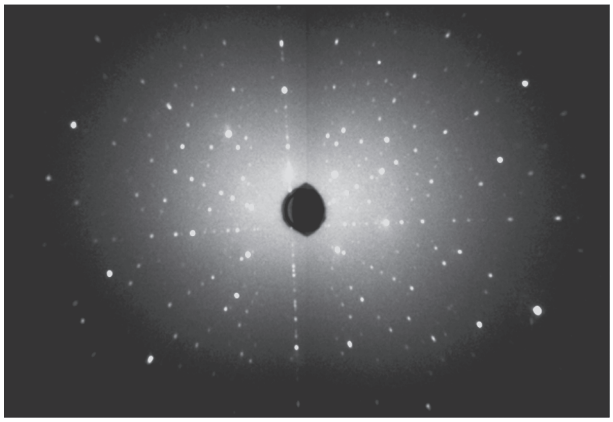

Fig. 2. Laue pattern of the $PbGa_{1-x}Fe_xBO_4$ single crystal for reflection from the (101) plane.

magnetic resonance (EPR) was measured on a Bruker Elexsys E-580 X-band spectrometer at room temperature. The first derivative of the absorption signal was recorded.

RESULTS

Figure 3 shows fragments of the EPR spectra recorded for three magnetic field orientations with respect to the crystal axes. Experimental spectrum *1* (thin black line) is recorded in a magnetic field parallel to the orthorhombic *b* axis. It has two narrow lines of different intensities. Spectrum *2* is recorded for a magnetic field normal to the *b* axis in a certain direction in the *ac* plane; at this field orientation, two groups of two narrow lines each of different intensities are observed. In addition, a narrow line, which was not identified, is also shown for this orientation at H = 3500 Oe. This line has a strong angular dependence of the resonance field and can be caused by an uncontrolled impurity of another paramagnetic ion or an iron ion with another valence. Spectrum *3* is recorded at an arbitrary magnetic field orientation; in this case, the group with the maximum signal intensity contains four lines. In addition, all three spectra (*1*–*3*) contain a broad line at H = 3500 Oe, which belongs to the holder of the sample.

The angular dependences of the resonance fields of individual lines of the EPR spectrum are obtained for two different planes of magnetic field rotation relative to the crystallographic axes. Figure 4 shows the angular dependences measured when a magnetic field rotates from the orthorhombic *b* axis to an arbitrary direction in the *ac* plane. The angular dependences during the rotation of a magnetic field in the *ac* plane are shown in Fig. 4b. Here, the open and solid circles represent the angular dependences for both high-intensity lines (Fig. 3, spectrum *2*), and blue triangles, for one of the low-intensity lines. Figure 4a depicts the angular dependence for only one of high-intensity spectral lines *2* in Fig. 3; it is marked with an asterisk. The open and solid blue triangles here correspond to low-intensity lines.

DISCUSSION

We now discuss the crystal structure of $PbGaBO_4$. The distortion of oxygen octahedra in $PbABO_4$ crystals depends on the A^{3+} ion, and some parameters of the octahedra are given in Table. 2. The oxygen environment is seen to be distorted most strongly in the $PbMnBO_4$ crystal, which is caused by the Jahn–Teller character of the Mn^{3+} ion [3, 5]. However, the oxygen octahedra in other crystals of the $PbABO_4$ family undergo noticeable distortions due to the influence of the binding groups BO_3 and PbO_4, and the octahedron distortions in $PbFeBO_4$ and $PbGaBO_4$ crystals are close in magnitude. In all $PbABO_4$ compounds, the character of distortion is such that the O3–A–O3 diagonal, which can be considered as a local axis of

Table 2. Crystal parameters of the oxygen octahedra in $PbABO_4$

Distance and angle	$PbFeBO_4$	$PbGaBO_4$	$PbMnBO_4$
A–O1, Å	1.923(3)	1.888(2)	1.885(3)
A–O2, Å	2.035(4)	2.008(2)	1.990(3)
A–O3, Å	2.095(4)	2.074(2)	2.225(4)
A–O1–A	101.2(2)°	102.55(16)°	104.0(2)°
A–O3–A	90.2(2)°	90.51(14)°	83.8(2)°

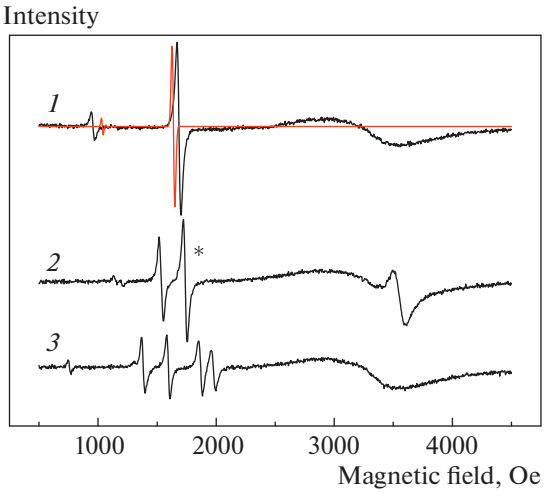

Fig. 3. EPR spectra of the Fe^{3+} ion recorded for the following three magnetic field orientations: (*1*) $H \parallel b$, (*2*) $H \perp b$, and (*3*) arbitrary orientation.

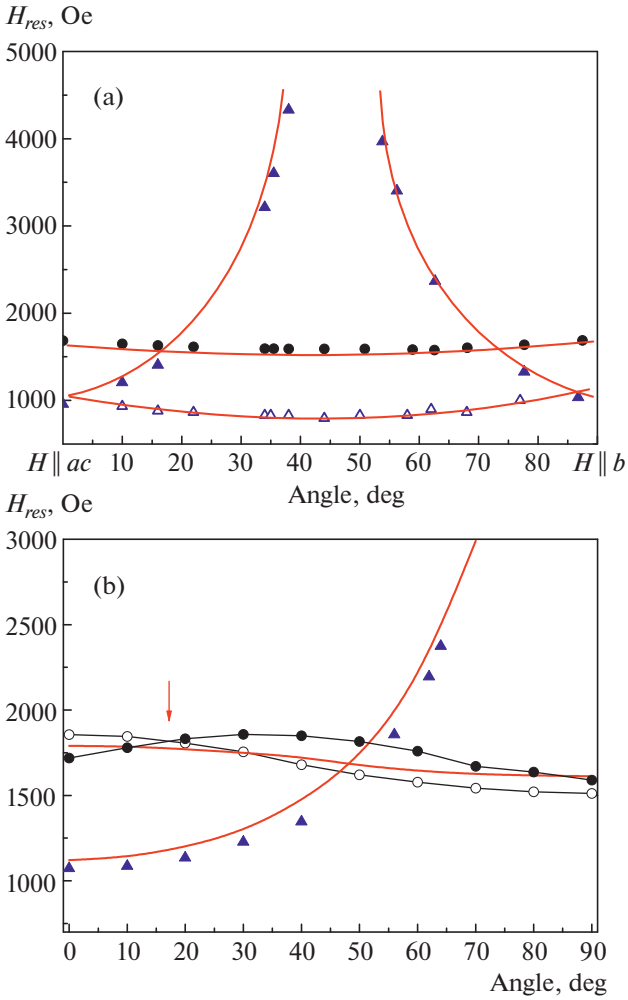

Fig. 4. Angular dependences of the resonance fields measured when a magnetic field is rotated (a) from the *b* axis to an arbitrary direction in the *ac* plane and (b) in the *ac* plane: (symbols) experiment and (solid lines) fitting with Hamiltonian parameters.

anisotropy for paramagnetic ions, is most strongly elongated in the octahedra [5, 7, 8]. Figure 5 shows fragments of the crystal structure of $PbGaBO_4$: two adjacent chains of octahedra are depicted, and the longest diagonals of the octahedra are indicated by heavy lines.

In each chain of the $PbGaBO_4$ crystal, the local axes of neighboring octahedra form an angle of 90.51° between them. Therefore, each local axis makes an angle of 44.7° with the orthorhombic *b* axis (see Fig. 5a). In addition, the local axes of each chain form a plane, and the planes of the local axes of neighboring chains rotate symmetrically about the *b* axis through an angle of ±31.3° with respect to the *a* axis (Fig. 5b).

These structural features allow us to explain the shape of the experimental EPR spectra at various magnetic field orientations. If we assume that the local axes of anisotropy of the Fe^{3+} ions substituting for Ga^{3+} ions in oxygen octahedra become the longest diagonals of the octahedra connecting the vertices with O3 ions, the shape of the EPR spectrum depends on the magnetic field orientation relative to these axes. Therefore, at an arbitrary field orientation, four most intense lines, which correspond to the four nonequivalent Fe^{3+} ion positions (with respect to the external magnetic field orientation) in the crystal, are observed in the EPR spectrum (Fig. 3, spectrum *3*). When a magnetic field is directed along the orthorhombic *b* axis, the local axes of all four nonequivalent Fe^{3+} ion positions are identically oriented with respect to a field (Fig. 5a). In this case, all four positions are degenerate and the EPR spectrum contains a single high-intensity line (Fig. 3, spectrum *1*). When a magnetic field is oriented in the *ac* plane, every pair of neighboring octahedra in a chain turns out to be degenerate. At the same time, the planes of the local axes of neighboring chains rotate through an angle of 62.6° with respect to each other; therefore, at an arbitrary field orientation in the *ac* plane, the spectrum has two high-intensity lines, each of which corresponds to Fe^{3+} ions in one of the chains (Fig. 3, spectrum *3*). When a field is oriented along the orthorhombic *a* or *c* axis, the corresponding spectrum degenerates into a single line, and one of the orientations is marked with a red arrow in Fig. 4b. This explanation is confirmed by comparing the EPR line intensities for different magnetic field orientations: the maximum intensity of a single EPR line is observed at $H \parallel b$, where all four Fe^{3+} ion positions are degenerate (Fig. 3, spectrum *1*), and the minimum line intensities correspond to an arbitrary magnetic field orientation (Fig. 3, spectrum *3*). The EPR spectra were analyzed using the XSophe software package [11] and the spin Hamiltonian written in the

approximation of the local orthorhombic symmetry of a paramagnetic center,

$$\hat{H} = -\hat{g}\beta SH + DS_z^2 + E(S_x^2 - S_y^2) + [B_4^0O_4^0 + B_4^2O_4^2 + B_4^4O_4^4]/60, \quad (1)$$

where $\hat{g}$ is the g factor tensor and b is the Bohr magneton. The form of spin operators O_4^0, O_4^2, and O_4^4 is given in [12]. The second, third and fourth terms in Eq. (1) describe the single-ion magnetic anisotropy of orthorhombic symmetry and determine the fine structure of the EPR spectrum for spin S. An analysis demonstrates that the most intense lines in the EPR spectrum are caused by transitions between the energy levels with $m = \pm 3/2$. Designation m used here instead of S reflects the fact that, as a result of action of the orthorhombic single-ion anisotropy, the initial "pure" wavefunctions of the doubly degenerate level with $S = \pm 3/2$ are mixed with the wavefunctions of the remaining levels with $S = \pm 1/2$ and $S = \pm 5/2$ taken with various weight coefficients. As a result, the transitions between the levels with $m = \pm 3/2$ and $m = \pm 5/2$ become allowed. The low-intensity lines belong to transitions with $m = \pm 1/2$ and $m = \pm 5/2$. The best fit of the experimental EPR spectra and their angular dependences using the XSophe software package gives the parameters given in Table 3.

The red line in Fig. 3 for spectrum *1* shows the single-ion EPR spectrum calculated taking into account the found parameters of spin Hamiltonian (1). The solid red lines in Fig. 4 depict the calculated angular dependences of the resonance fields of the single-ion EPR spectrum calculated using the parameters from Table. 3. In all cases, good agreement with the experimental results is observed. In Fig. 4, calculated angular dependencies (red lines) are shown only for one of the chains. As follows from an analysis of the crystal structure (Fig. 5b), the similar angular dependencies obtained for the other chain should be shifted by an angle of 62.6° relative to the first chain. In the experiment, this angle turned out to be approximately 40°. A comparison with the experimental angular dependence for one of the high-intensity lines (open circles) also demonstrates that the dependences coincide qualitatively, but the amplitude of the experimental dependence is approximately one and a half times higher than that of the calculated dependence. These discrepancies are thought to be explained by the inaccuracy of the sample orientation. The obtained values of the single-ion anisotropy constants are unusually high for the Fe^{3+} ion, which is an S ion in the free state. In most crystals, the value of constant D for this ion does not exceed 0.1–0.2 cm^{-1}. For example, the single-ion anisotropy constant of an Fe^{3+} ion in a diamagnetic $CaCO_3$ crystal, the nearest environment of which is an oxygen octahedron with weak trigonal distortions, is $D = 0.0922 \pm 0.0003$ cm^{-1} [13, 14]. Strong distortions of the oxygen environment, including oxygen vacancies, lead to significant values of single-ion anisotropy constant D, which vary within 0.67–4.38 cm^{-1} for a number of diamagnetic crystals, for this ion [15–18]. Thus, the strong single-ion magnetic anisotropy of the Fe^{3+} ion in the $PbGaBO_4$ crystal is also a consequence of strong distortions of the oxygen environment of the ion in this crystal. The single-ion contribution to the energy of the total magnetic anisotropy of a magnetically concentrated crystal can be estimated in the approximation of a classical collinear magnet with moments oriented along the orthorhombic axes of the $PbFeBO_4$ lattice. Using the single-ion

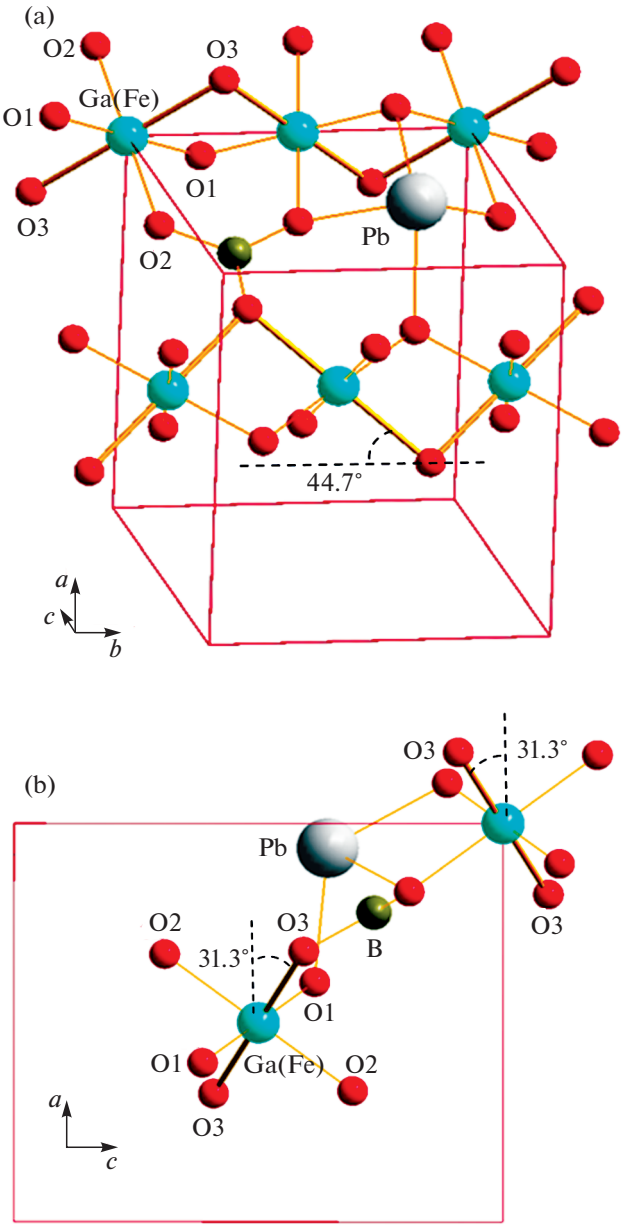

Fig. 5. Fragment of the crystal structure of $PbGaBO_4$ containing two neighboring chains of octahedra: (a) general view and (b) view along the orthorhombic b axis.

Table 3. Fitting parameters of spin Hamiltonian (1)

g_x	g_y	g_x	D, cm^{-1}	E, cm^{-1}	B_4^0, cm^{-1}	B_4^2, cm^{-1}	B_4^4, cm^{-1}
1.8(1)	2.0(1)	1.9(1)	−2.57(5)	0.95(5)	0.41(4)	1.30(8)	0.94(3)

anisotropy parameters found from the EPR spectra (Table 3), we obtain the energy per spin to within an additive constant, $E_a \approx -1.44S^2\ cm^{-1}$, $E_b \approx -1.19S^2\ cm^{-1}$, and $E_c \approx -0.86S^2\ cm^{-1}$.

Thus, the obtained single-ion anisotropy parameters demonstrate that the orthorhombic axis *a* as a common easy magnetization axis and the *c* axis is a hard magnetization axis. It is these directions of easy and hard magnetization axes that form in a $PbMnBO_4$ ferromagnet [5]. The *a* axis in a $PbCrBO_4$ antiferromagnet is also an easy magnetization axis [3]. In addition, the data of neutron and magnetic measurements [3, 4] demonstrate that the orthorhombic *c* axis in magnetically concentrated $PbFeBO_4$ is the easy anisotropy axis. When describing the spin-wave spectrum of $PbFeBO_4$, Prosnikov [19] took into account the magnetic anisotropy of the crystal with a macroscopic easy anisotropy axis, which also coincides with the orthorhombic *c* axis. This discrepancy between the experimentally found orientation of the easy anisotropy axis in $PbFeBO_4$ and the easy axis direction for the single-ion mechanism can be competition with dominant two-ion mechanisms of the Fe–Fe interaction anisotropy, which define the *c* axis as an effective easy axis in the crystal. An anisotropic exchange interaction is likely to be such a two-ion dominant mechanism, which is indicated by the anisotropy of the paramagnetic Curie temperature in $PbFeBO_4$ [4].

CONCLUSIONS

Crystals of a diamagnetic $PbGaBO_4$ analog containing a small amount (about 0.5 at %) of Fe^{3+} ions, which are optimal for recording a single-ion EPR spectrum, were grown. Their EPR spectra were analyzed with allowance for a crystal structure, and the existence of four Fe^{3+} ion positions with different local anisotropy axis directions, which are nonequivalent with respect to the orientation of an applied magnetic field, was confirmed. The shape of the EPR spectra and the angular dependences of the resonance fields are determined by the magnetic field directions relative to local anisotropy axes, which coincide with the longest diagonals of the oxygen ion octahedra surrounding Fe^{3+} ions. The most intense lines of the EPR spectra were shown to be caused by transitions between the levels with $m = \pm 3/2$, and the low-intensity lines in the spectra belong to the transitions with $m = \pm 1/2$ and $m = \pm 5/2$. The experimental data were analyzed in terms of a spin Hamiltonian written in the approximation of the local orthorhombic symmetry of a paramagnetic center. The parameters of the spin Hamiltonian were determined from the fitting of the experimental EPR spectra and their angular dependences. The values of the found parameters of single-ion anisotropy are unusually high for the Fe^{3+} ion and are caused by strong distortions of the oxygen environment of the ions in the $PbGaBO_4$ lattice. The estimated single-ion contribution to the energy of the total magnetic anisotropy in the magnetically concentrated $PbFeBO_4$ antiferromagnet demonstrates that the orthorhombic *a* axis is a common easy axis and the *c* axis is a hard axis. However, as follows from the experimental data, the magnetic anisotropy of this crystal is characterized by an easy axis coinciding with the orthorhombic *c* axis. This discrepancy between the easy axes can be competition with dominant two-ion mechanisms of the Fe–Fe interaction anisotropy, which define the *c* axis as an effective easy axis in the crystal.

ACKNOWLEDGMENTS

We are grateful to M.S. Pavlovskii for measuring the Laue patterns of the $PbGaBO_4$ crystal.

FUNDING

This work was supported by the Russian Foundation for Basic Research, the Government of the Krasnoyarsk Territory, and the Krasnoyarsk Regional Science Foundation (project No. 20-42-240006 "Synthesis and study of oxide single crystals containing Pb^{2+} and Bi^{3+} with partial substitution in one of the subsystems: magnetic structures and magnetodielectric effect").

REFERENCES

1. H. Park and J. Barbier, Acta Crystallogr. E **57**, i82 (2001).
2. H. Park, J. Barbier, and R. P. Hammond, Solid State Sci. **5**, 565 (2003).
3. H. Park, R. Lam, J. E. Greedan, and J. Barbier, Chem. Mater. **15**, 1703 (2003).
4. A. Pankrats, K. Sablina, D. Velikanov, et al., J. Magn. Magn. Mater. **353**, 23 (2014).
5. A. Pankrats, K. Sablina, M. Eremin, et al., J. Magn. Magn. Mater. **414**, 82 (2016).
6. A. Pankrats, M. Kolkov, S. Martynov, et al., J. Magn. Magn. Mater. **471**, 416 (2019).
7. A. Pankrats, M. Kolkov, A. Balaev, et al., J. Magn. Magn. Mater. **497**, 165997 (2020).

8. S. N. Martynov, Phys. Solid State **62**, 1165 (2020).
9. S. N. Martynov, Phys. Solid State 63 (2021, in press).
10. J. Head, P. Manuel, F. Orlandi, et al., Chem. Mater. **32**, 10184 (2020).
11. M. Griffin, A. Muys, C. Noble, et al., Mol. Phys. Rep. **26**, 60 (1999).
12. A. Abragam and B. Bleaney, *Electron Paramagnetic Resonance of Transition Ions* (Oxford Univ., London, 1970), Vol. 2.
13. J. Wakabayashi, J. Chem. Phys. **130**, 144 (1963).
14. V. A. Atsarkin, V. G. Lushnikov, and L. P. Sorokina, Sov. Phys. Solid State **7**, 1912 (1965).
15. D. L. Carter and A. Okaya, Phys. Rev. **118**, 1485 (1960).
16. H. Unoki and T. Sakudo, J. Phys. Soc. Jpn. **23**, 546 (1967).
17. E. S. Kirkpatrick, K. A. Muller, and R. S. Rubins, Phys. Rev. **135**, A86 (1964).
18. P. Eisenberger and P. S. Pershan, J. Chem. Phys. **45**, 2832 (1966).
19. M. A. Prosnikov, Phys. Rev. B **103**, 094443 (2021).

Translated by K. Shakhlevich

SPELL: OK